ON THE PERFORMANCE OF SPECTRALLY EFFICIENT CPM-OFDMA FOR AERONAUTICAL TELEMETRY

Marilynn Wylie
Glenn Green
Gem Direct Inc.
Irving, TX 75063
ggreen@gemdirect.org
*

ABSTRACT

In this paper, we discuss CPM-OFDMA (Continuous Phase Modulation - Orthogonal Frequency Division Multiple Access) - a novel modulation that maps a discrete-time CPM into a spectrally efficient DFT-spread OFDMA transmission. Three CPM-OFDMA schemes are developed based on discrete-time variants of PCM/FM, SOQPSK-TG and ARTM-CPM telemetry modulations. Simulations reveal that spectrally efficient CPM-OFDMA schemes can outperform the conventionally defined telemetry schemes in the AWGN environment. For example, maximum likelihood sequence detection of conventional PCM/FM yields a BER of 10^{-5} at an E_b/N_0 of 8.4 dB while the least complex CPM-OFDMA scheme that is based on sampling a PCM/FM waveform once per symbol interval achieves the same BER at an E_b/N_0 of 7.8 dB. Finally, an extensive search to find a subset of the best performing binary schemes shows that there exist very low complexity schemes that can achieve a BER of 10^{-6} at an E_b/N_0 of 7.8 dB, which is an order of magnitude improvement over the performance of PCM/FM at the same E_b/N_0.

INTRODUCTION

Over the past forty years, the requirements of aeronautical telemetry systems have evolved from data rates in the neighborhood of 100s of kbits/sec in the 1970s to the current demand for 10-20 Mbits/sec. Consequently, increased spectral efficiency and frequency agility have recently been identified as key enablers for sustaining the applications and services that are needed to support data-intensive test flight missions and multi-user access to the telemetry band.

From a historical perspective, PCM/FM (Tier 0) has been the primary modulation of choice in aeronautical telemetry for the past forty years. However, the demand for higher data rate testing over the allocated L-band (1435 - 1535 MHz), the lower S-band (2200 - 2290 MHz) and the upper S-band (2310 - 2390 MHz) as well as the reallocation of the lower portion of the upper S-band from 2310 - 2360 MHz to other services imposed a requirement to identify alternate CPM waveforms possessing higher spectral efficiency than PCM/FM.

*This work was supported by the Test Resource Management Center (TMRC) Test and Evaluation Science and Technology (T&E/S&T) Program through a Grant from the Army PEO STRI Contracting Office under Contract No.W900KK-10-C-0017. Approved for Public Release, Distribution is Unlimited, AFFTC-PA-10383.

In response, the Advanced Range Telemetry (ARTM) program [1] was instituted in order to identify modulation schemes that required less bandwidth than PCM/FM but which had the same detection efficiency. One of the newly identified waveforms, SOQPSK-TG (Tier 1) (Shaped Offset Quadrature Phase Shift Keying-TG) [2], has the same detection efficiency as PCM/FM but twice the spectral efficiency whilst a second waveform (called ARTM-CPM) [3], has the same detection efficiency as PCM/FM but three times its spectral efficiency [4].

Even with the three-fold advance in spectral efficiency with the adoption of ARTM-CPM, today's aeronautical telemetry systems remain constrained by the use of single-carrier modulations that require the use of guard bands between adjacent channels. Thus, the current protocol does not permit a frequency agile use of the radio spectrum and there is still some loss in spectral efficiency from the loss in system capacity that is due to the presence of guard bands. For example, the minimum required separation between two 10 Mbits/sec ARTM CPM waveforms is 9 MHz [5] to allow adequate channel separation. Furthermore, as stated in the IRIG-106 standards, [5], "the simultaneous operation of multiple emitters that are co-located, with similar power levels and transmitting antenna direction is done by separating them by a guard band that is greater than or equal to the occupied bandwidth of the widest bandwidth signal".

In this paper, we discuss CPM-OFDMA, a robust modulation that is developed based on the salient observation that the samples from a discrete-time equivalent CPM waveform can be substituted for the conventional BPSK, QPSK and M-QAM symbols in a DFT-spread OFDMA transmission [6]. Hence, power efficient CPM-like schemes can be transmitted over the radio spectrum in spectrally efficient OFDMA style. This empowers the telemetry spectrum manager to allow different users to cooperatively *share* resources without harmfully interfering with each other. In addition, CPM-OFDMA mitigates the need for instituting multiple guard bands to reduce co-channel interference, since CPM-OFDMA waveforms from different users are transmitted over *orthogonal* subcarriers. Hence, there is the potential to increase the spectral efficiency of the telemetry system while maintaining a physical layer dependence on the core underlying waveforms (e.g., PCM/FM, ARTM-CPM and SOQPSK-TG). Hence, CPM-OFDMA is seen as a complementary technology that may serve as an alternative physical layer modulation when heavily congested or contended spectrum access makes spectral efficiency and/or frequency agility an overriding concern.

The two main contributions of this paper are as follows -

- The identification and performance analysis of of three CPM-OFDMA schemes that are developed based upon the manipulation of conventional PCM/FM, ARTM-CPM and SOQPSK-TG. In this study we not only show that some CPM-OFDMA schemes can offer *equivalent* performance to their conventional counterparts, but that the most spectrally efficient CPM-OFDMA schemes (requiring only one sample per symbol interval of the underlying CPM waveform) can offer *significantly better* BER performance in the AWGN environment.

- The identification of a subset of spectrally efficient, low state complexity binary CPM-OFDMA schemes that offer superior performance in the AWGN environment when compared to their conventional CPM counterparts. In fact, when compared to the performance of conventional PCM/FM, the best of these schemes offers an *order of magnitude* improvement in receiver performance at a target BER of 10^{-6}.

SIGNAL MODEL

In the most general scenario, we consider a multi-user system in which there are U users that transmit simultaneously across a swathe of the available radio spectrum using CPM-OFDMA waveforms. The complex baseband equivalent symbols that are generated by the u^{th} user ($u = 0, \cdots, U-1$) are derived from the sampled outputs from an underlying continuous-time CPM waveform.

In this study, we presume a data frame that is constructed from the observation of a JT second CPM waveform, where T denotes the symbol interval and J denotes an integral number of symbol intervals. The waveform is sampled at a rate of N times per symbol interval, thus resulting in a length-JN vector of signal samples

$$\boldsymbol{s}_u = \begin{bmatrix} s_{u,0} & \cdots & s_{u,JN-1} \end{bmatrix}^T. \tag{1}$$

The signal samples in $\mathbf{s}_u$ represent the discrete-time model of the CPM waveform, $s_u(t;\beta_u)$, i.e., $s_{u,iN+m} = s_u(t;\boldsymbol{\beta}_u)|_{t=iT+\frac{m}{N}T}$ for $i = 0, \cdots, J-1$ and $m = 0, \cdots, N-1$. The complex baseband equivalent CPM waveform is defined as

$$s_u(t;\boldsymbol{\beta}_u) = e^{j\phi_u(t;\boldsymbol{\beta}_u)} \tag{2}$$

where the phase is of the form

$$\phi_u(t;\boldsymbol{\beta}_u) = 2\pi \sum_i h_{\underline{i}} \beta_{u,i} q(t - iT). \tag{3}$$

Associated with the u^{th} waveform are the following: $\beta_{u,i}$ denotes the ith M-ary symbol, T is the symbol duration. $h_{\underline{i}}$ is the digital modulation index which cycles, in a roundrobin fashion, from one symbol interval to the next over the members of a set, $\mathbf{S}$, of cardinality H. Hence, we can define $\mathbf{S} = \begin{bmatrix} h_0 & \cdots & h_{H-1} \end{bmatrix}$. The rule $\underline{i} = i \mod H$ maps the index of the current symbol interval to member of the set using modular arithmetic. In a single-h system, $H = 1$, whilst for multi-h schemes, $H > 1$.

The phase response $q(t)$ is usually defined as the time-integral of a frequency pulse $F(t)$ with area $1/2$, i.e.

$$q(t) = \begin{cases} 0 & t < 0 \\ \displaystyle\int_0^t F(\lambda)\, d\lambda & 0 \le t < LT \\ \frac{1}{2} & t \ge LT \end{cases} \tag{4}$$

where L denotes the frequency pulse length, expressed in an integer number of symbol durations. When $L = 1$ the signal is *full response* and when $L > 1$ the signal is *partial response*.

Three CPM-based waveforms that are widely used in aeronautical telemetry and which are considered in this study correspond to ARTM-CPM, PCM/FM and SOQPSK-TG. Both ARTM-CPM and PCM/FM use the raised cosine frequency pulse of duration LT, (denoted LRC) which is defined as

$$F_0(t) = \begin{cases} \frac{1}{2LT}\left[1 - \cos\left(\frac{2\pi t}{LT}\right)\right] & 0 \le t < LT \\ 0 & \text{otherwise.} \end{cases} \tag{5}$$

SOQPSK-TG utilizes a special waveform, $F_1(t)$, that is defined as

$$F_1(t) = A \frac{\cos(\pi\rho B t)}{1 - 4\left(\frac{\rho B t}{2T}\right)^2} \cdot \frac{\sin\left(\frac{\pi B t}{2T}\right)}{\left(\frac{\pi B t}{2T}\right)} \cdot w(t) \tag{6}$$

where the windowing function, $w(t)$, is defined as

$$w(t) = \begin{cases} 1 & 0 \leq \left|\frac{t}{2T}\right| \leq T_1 \\ \frac{1}{2} + \frac{1}{2}\cos\left(\frac{\pi}{T_2}\left(\frac{t}{2T} - T_1\right)\right) & T_1 \leq \left|\frac{t}{2T}\right| \leq T_1 + T_2 \\ 0 & T_1 + T_2 < \left|\frac{t}{2T}\right| \end{cases} . \quad (7)$$

The additional parameters that are defined for the SOQPSK-TG waveforms are given by: $T_1 = 1.5$, $T_2 = 0.5$, $\rho = 0.7$ and $B = 1.25$ and the normalization constant A is defined such that the phase response function, $q_1(t) = \int_0^t F_1(\lambda)d\lambda = \frac{1}{2}$ for $t > LT$.

During the interval corresponding to the nth symbol, $nT \leq t < (n+1)T$, the phase in (3) may be expressed as

$$\phi_u(t; \boldsymbol{\beta}_u) = \underbrace{2\pi \sum_{i=n-(L-1)}^{n} h_{\underline{i}} \beta_{u,i} q(t - iT)}_{\theta_u(t; \boldsymbol{\beta}_{u,n})} + \underbrace{\pi h \sum_{i=0}^{n-L} \beta_{u,i}}_{\phi_{u,n-L}} \quad (8)$$

where $\boldsymbol{\beta}_{u,n} = \left\{\beta_{u,n-(L-1)}, \cdots, \beta_{u,n}\right\}$ is the correlative state vector which contains the $L-1$ past symbols and the current input symbol. These L symbols determine the phase trajectory taken by $\theta_u(t; \boldsymbol{\beta}_{u,n})$ in (8) during the interval $nT \leq t \leq (n+1)T$. There are M^L possible values the correlative state vector can assume, each resulting in a different phase trajectory.

The second term in (8), $\phi_{u,n-L}$, is called the cumulative phase and represents the contribution of all symbols that have worked their way through the time-varying portion of the phase response in (4) and thus contribute a constant value to the overall phase. When the set $\boldsymbol{S}$ of modulation indices contains all rational entries, then the cumulative phase $\phi_{u,n-L}$ is drawn from a finite alphabet. In this case, the CPM signal can be described as a finite state machine, with a corresponding trellis diagram, and a maximum likelihood sequence detection (MLSD) scheme can be implemented using the Viterbi algorithm (VA) [7].

OVER THE AIR TRANSMISSION OF CPM-LIKE SIGNALS USING OFDMA

The modulated data symbols that are used in contemporary DFT-spread OFDMA systems are typically drawn from BPSK, QPSK or M-QAM constellations. However, as stated in this paper we consider modulated data symbols that are obtained from the *sampled output* of a CPM modulator. As we now show, beyond the obvious differences in data symbol generation between conventional OFDMA and CPM-OFDMA, the remaining transmitter operations are equivalent.

In what follows, we consider the downlink, wherein users map their data to an assigned subset of the available subcarriers and transmit to a common receiver (eg., from the test article to the ground station). Although not addressed in this paper, similar concepts may be applied for an uplink CPM-OFDMA transmission.

In this scenario, there is a total of K subcarriers over the entire band, JN of which are allocated to the u^{th} user. The time domain signal vector is transformed into the frequency domain by means of the JN-point DFT (Discrete Fourier Transform) to yield the frequency domain coefficients:

$$S_{u,i} = \sum_{n=0}^{JN-1} s_{u,n} e^{-j2\pi in/JN} \quad (9)$$

where $i = 0, \cdots, JN-1$ denotes the discrete frequency index. Assuming that K is an integer multiple of JN, and that the DFT coefficients of each user are mapped at regular intervals (i.e., *interleaved*) across the frequency band, the mapped coefficients can be expressed as

$$\tilde{S}_{u,k} = \begin{cases} S_{u,i} & k = u + iU \\ 0 & \text{otherwise} \end{cases} \tag{10}$$

for $i = 0, \cdots, JN-1$ and $u \in \{0, \cdots, U-1\}$.

Once mapped to the desired set of subcarriers, the frequency domain coefficients in (10) are transformed back into the time domain by means of the K-point IDFT (Inverse DFT) operation ($K = UJN$), which yields

$$\tilde{s}_{u,n} = \frac{1}{UJN} \sum_{k=0}^{UJN-1} \tilde{S}_{u,k} e^{j2\pi kn/UJN}. \tag{11}$$

Now, making the substitution $k = u + iU$ to extract the data from thte u^{th} user, it can be shown that

$$\tilde{s}_{u,n} = \left(\frac{1}{UJN} \sum_{i=0}^{JN-1} S_{u,i} e^{j2\pi in/JN} \right) e^{j2\pi un/UJN} \tag{12}$$

which demonstrates that the original input sequence, $s_{u,n}$, is scaled and repeated U times in the post-IDFT sequence, $\tilde{s}_{u,n}$, i.e.

$$\tilde{s}_{u,n} = \frac{1}{U} s_{u,\underline{n}} e^{j2\pi un/UJN} \tag{13}$$

where the underlined time index, defined as $\underline{n} \triangleq n \bmod JN$, captures the effect of the U repetitions. We use $\tilde{\boldsymbol{s}}_u$ to denote the vector of post-IDFT samples.

The fundamental observation is that since the CPM-OFDMA symbols, $\tilde{s}_{u,n}$, are constant envelope, the post-IDFT sequence will also be constant modulus and will therefore be amenable to the use of nonlinear power amplification in the more power efficient region of operation (saturation). We note that some of that power efficiency may be lost if the post-IDFT samples are passed through a transmission filter in order to meet spectral mask requirements. However, based on studies (not elaborated in this paper), the loss in power efficiency may be minor depending on the filter characteristics.

PARAMETERIZATIONS OF PCM/FM, SOQPSK-TG and ARTM CPM

In the preceding sections of this paper, we have provided the complete derivation of CPM-OFDMA. As shown, it is a straightforward extension of CPM that facilitates an OFDMA-style transmission. Given our references to PCM/FM, ARTM-CPM and SOQPSK-TG throughput, the next natural question is: *How do the CPM-OFDMA variants of these waveforms perform in comparison to their conventionally defined counterparts*? Thus, the objective of our first numerical study (presented in a later section) is to address that question by defining the family of CPM-OFDMA waveforms that can be derived based on these three telemetry modulations and then presenting the results of numerical simulations to determine their BER performances in the AWGN channel.

Binary PCM/FM can be modeled as a single-h, partial response CPM waveform in which the modulation index $h = 7/10$, the signal memory $L = 2$ and $M = 2$. The frequency pulse is a raised cosine. Hence PCM/FM is shortly described as a 2RC CPM.

ARTM-CPM is a quatenary ($M = 4$), partial response 2-h CPM wherein the digital modulation indices are defined as $h_{\underline{0}} = 4/16$ and $h_{\underline{1}} = 5/16$. Since $L = 3$ and the raised cosine frequency pulse is used, we can shortly denote it as a 3RC waveform. .

SOQPSK-TG is a single-h partial response CPM in which the modulation index $h = 1/2$ and $L = 8$. It is unique and distinguishable from PCM/FM and ARTM-CPM, in that it is a ternary CPM ($M = 3$) that uses a precoder to convert the binary data $b_{u,n} \in 0, 1$ into ternary data, $\beta_{u,n}$ according to the mapping $\beta_{u,n} = (-1)^{n+1} (2b_{u,n-1} - 1) (b_{u,n} - b_{u,n-2})$. Hence, $\beta_{u,n} \in \{-1, 0, 1\}$. The precoder is always dependent on the two previous input bits.

It has been shown [8] that the two oldest bits map to the phase state of the SOQPSK-TG CPM waveform. In fact, there is a one-to-one mapping between the set of possible state variables, $S_n = \{00, 01, 10, 11\}$ and the SOQPSK-TG phase states: $\theta_{n-8} \in \{0, \pi/2, \pi, 3\pi/2\}$. This mapping is given by $\left\{00 \leftrightarrow \frac{3\pi}{2}; 01 \leftrightarrow \pi; 10 \leftrightarrow 0;\ 11 \leftrightarrow \frac{\pi}{2}\right\}$. By convention, the first symbol in S_n conveys the symbol that appeared during the oldest even symbol interval and the second symbol in S_n conveys the symbol that appeared in the oldest odd symbol interval. By its definition, SOQPSK-TG admits a time-varying trellis description, which has been treated in previous publications [8].

PCM/FM, ARTM-CPM and SOQPSK-TG can all be easily mapped into CPM-OFDMA waveforms by sampling in the time domain and then mapping the time domain samples to the frequency domain for subcarrier allocation. The resulting time-domain CPM-OFDMA signals have the same trellis description as their conventionally defined counterparts, and hence the same algorithms can be applied at the receiver with unaltered complexity.

MAXIMUM LIKELIHOOD SEQUENCE DETECTION

When the transmitted signal passes through an AWGN channel, the total received signal on the downlink from all of the users is $r_n = \sum_{u=0}^{U-1} \tilde{s}_{u,n} + w_n$ where w_n denotes complex-valued AWGN with zero mean and one-sided PSD N_0. The portion of the signal that is transmitted by the desired (u^{th}) user may be extracted by first transforming r_n into the frequency domain via the DFT operation $\tilde{R}_k \xleftarrow{\text{DFT}} r_n$ and then extracting those coefficients of $\tilde{R}_k$ that correspond to the uth user's assigned frequencies. We obtain the uth time-domain signal as $R_{u,i} \xrightarrow{\text{IDFT}} r_{u,n}$. The information symbols for the uth user are detected by processing $r_{u,n}$ using the well-known VA, which performs MLSD by correlating $r_{u,n}$ against all possible transmitted signals and returning the information sequence with the maximum correlation, cf. e.g. [7].

NUMERICAL STUDY AND DISCUSSION

In this first study, we compare the BER performance of CPM-OFDMA schemes that are based on PCM/FM, ARTM-CPM and SOQPSK-TG to their conventional counterparts. In addition, we investigate the impact of the sample rate, N, on CPM-OFDMA performance. In all cases, a single user transmits in the AWGN channel environment. In the construction of the CPM-OFDMA waveforms, we have selected the sample rate of the underlying CPM as either $N = 1$, $N = 2$ or $N = 4$. However, the conventional PCM/FM, ARTM-CPM and SOQPSK-TG schemes are simulated by setting $N = 16$ samples per symbol interval. This high sampling rate allows us to generate a waveform that very closely approximates the characteristics of a continuous-time CPM.

First, we compare the uncoded BER performance of conventional PCM/FM to that of the three CPM-

OFDMA schemes that are derived by allowing $N = 1$, $N = 2$ and $N = 4$. The results are depicted in Figure (1). Here, it is shown that for $N \geq 2$, that the performance of the CPM-OFDMA schemes are actually *equivalent* to that of conventional PCM/FM. Hence, there is *no* discernable loss in BER performance by implementing the CPM-OFDMA counterpart of PCM/FM. For the special case wherein $N = 1$, we actually achieve superior performance to all of the other schemes, as illustrated by the 0.6 dB gain in performance of the CPM-OFDMA ($N = 1$) at a BER of 10^{-5}. Hence, in this case, it is conceivable that we can send *only one* sample per symbol interval of the sampled PCM/FM waveform, which is highly desirable from the stance of achieving higher spectral efficiency by using fewer subcarriers.

In this next study, we compare the BER performance of cnventional ARTM-CPM to that of three CPM-OFDMA schemes that are constructed by sampling a ARTM-CPM waveform. The outcome of this investigation is graphically illustrated in Fig. (2), where it is evident that the conventional ARTM-CPM waveform performs fractionally worse than all of the other schemes at a BER of 10^{-5}. The trend observed from these results is that the performance of the CPM-OFDMA scheme actually shows moderate improvement as the sample rate, N, is *decreased*, with the best overall performance achieved for the case wherein $N = 1$. At a BER of 10^{-5}, the $N = 1$ scheme has 0.9 dB advantage over the conventionally defined ARTM-CPM waveform. This result argues that there exists a spectrally efficient ($N = 1$) implementation of ARTM-CPM based CPM-OFDMA that also demonstrates good performance over the AWGN channel.

In the final study, we compare the BER performance of conventional SOQPSK-TG to that of three CPM-OFDMA schemes that are constructed by sampling the ARTM-CPM waveform at a rate of $N = 1$, $N = 2$ or $N = 4$ times per symbol interval. The results of this study are shown in Fig. (3). Our results indicate that for $N \geq 2$, the BER performance of the CPM-OFDMA schemes is equivalent to that of conventional SOQPSK-TG. Hence, there is *no* performance loss incurred by the use of SOQPSK-TG-based CPM-OFDMA. However, there is a *slight* loss in performance for $N = 1$. At a BER of 10^{-5}, we observe a 0.4 dB loss when using the $N = 1$ CPM-OFDMA scheme, as compared to the conventional and other CPM-OFDMA schemes ($N = 2$ and $N = 4$). Hence, there is the possibility to leverage the increase in spectral efficiency versus a slight loss in performance in the selection of $N = 1$. An open question involves understanding why the performance for $N = 1$ exhibits such behavior given that we have seen the opposite behavior for the PCM/FM and ARTM-CPM based modulations, and whether it is related to the introduction of the precoder or if there are other signal characteristics that are relevant. That remains the focus of current study.

In this second study, we highlight the outcome of an optimization study that has identified a *subset* of the best performing binary, single-h LRC CPM-OFDMA schemes in the AWGN environment. The objective of this study is to identify other binary schemes that are based on CPMs that are not used for aeronautical telemetry but which can deliver good BER performance and spectral efficiency. The search space is constrained to all combinations of the following parameter sets: modulation index h, signal memory, L and signal sampling rate, N. In all cases $M = 2$. $\boldsymbol{h} = \left\{\frac{m}{n}\right\}$, $\boldsymbol{L} \in \{2, 3, 4\}$ and $\boldsymbol{N} \in \{1, 2, 4, 8, 16\}$. m and n are all co-prime integers in the set $m \in \{1, ..., 9\}$ and $n \in \{2, ..., 10\}$ with $m < n$.

Of the entire survey of 372 different CPM-OFDMA schemes, there are several that clearly dominated our findings and their performance is highlighted in this section. In general, we make the comment that as the modulation index approaches unity (e.g., $h = 8/9$), that the BER performance improves relative to those schemes that use a smaller value of the modulation index (e.g., $h = 1/10$). In addition, we generally observe that for $L = 2$, that the best performing CPM-OFDMA schemes can be implemented with $N = 1$. However, for $L = 3$, the CPM-OFDMA schemes that utilize a sampling rate of $N = 1$ are actually the

Table 1: Subset of Best Performing Binary CPM-OFDMA Schemes. (E_b/N_0 (dB) at a BER of 10^{-6}).

	$L=4$, $N=1$	$L=4$, $N=1$	$L=3$, $N=2$	$L=3$, $N=2$	$L=3$, $N=1$	$L=2$,$N=1$	$L=2$,$N=1$
h	Num. States	E_b / N_0	Num. States	E_b / N_0	E_b / N_0	Num. States	E_b / N_0
3/4	-	-	16	8.8	9.2	-	-
4/5	45	8.4	20	8.6	9.0	-	-
5/6	48	8.4	24	8.4	8.8	12	7.8
6/7	56	8.1	28	8.2	8.8	14	7.8
7/8	64	8.1	32	8.2	8.8	16	7.8
7/9	-	-	-	-	-	18	8.0
8/9	72	8.0	36	8.3	8.8	18	8.0
9/10	80	8.0	40	8.3	8.8	20	8.0

worst performing schemes (compared to their counterparts that use higher sampling rates). Finally, when $L = 4$, CPM-OFDMA becomes rather insensitive to the sampliing rate of the underlying CPM waveform as the BER performance for all cases ($N = 1$, $N = 2$, $N = 4$ and $N = 8$) are close. Space limitation preclude graphical BER plots. However the results are summarized in Table(1).

The modulation indices of the six best performing binary CPM-OFDMA schemes for $L = 2$ are shown in Table (1). The simulation reveal that for $N = 1$, that all of these schemes reach a target BER of 10^{-6} at an E_b/N_0 range of 7.8 - 8.0 dB. The state complexity for each scheme, which is defined as pM^{L-1} (where p denotes the denominator of the modulation index) and the Eb/No (dB) at which the target BER of 10^{-6} is achieved are shown in Table (1).

We now discuss the performance of the best $L = 3$ RC binary CPM-OFDMA schemes. In this case, the optimal modulation index set is defined in Table (1). A notable observation is that relative to our findings for $L = 2$, we have additional modulation indices in the optimal set that have lower values (e.g., $h = 3/4$). The BER performance reveals that for $L = 3$ and $N = 1$, the CPM-OFDMA schemes are only slightly outperformed by the schemes that utilize higher sampling rates ($N = 2$, $N = 4$, $N = 8$ and conventional CPM). It is at most 0.5 dB at a BER of 10^{-6}. For the schemes wherein $N > 1$, the target BER of 10^{-6} is generally reached within an E_b/N_0 range of 8.2 - 8.8 dB. In Table (1), we show the performance and state complexity of the best schemes for $N = 1$ and $N = 2$, as these represent the most spectrally efficient and best performing CPM-OFDMA schemes, respectively when $L = 3$. A direct comparison of the results for $L = 2$ that are shown in Tables (1) reveals the 1 dB improvement in performance at a BER of 10^{-6} when the memory of the signal increases from $L = 2$ to $L = 3$. Hence, one can trade off the moderately higher complexity for a better BER performance. It is very important to bear in mind, however, that all of these schemes require low complexity at the receiver (the most complex scheme for $L = 3$ having 40 states in its trellis).

Finally, we discuss BER performance of the six best performing binary schemes for $L = 4$. Their corresponding modulation indices are shown in Table (1). We have observed that the performance of all of these schemes is rather insensitive to the sampling rate of the underlying CPM waveform. In this case, we have only simulated to a target BER of 10^{-5} and so we provide an extrapolated estimate of the performance at 10^{-6} in Table (1).

In this final study, we demonstrate the BER performance of CPM-OFDMA in a multi-user environment in which $U = 4$ users simultaneously transmit four independently generated CPM-OFDMA waveforms by sampling a PCM/FM waveform at the rate of $N = 1$ sample per symbol interval. The DFT coefficients of each user are regularly interleaved across the radio band. Each user generates $J = 256$ bits per trans-

mission interval. Hence, the total IDFT size is $UJN = 1024$. The superimposed signal from the four users is measured at the receiver, which detects the signal that is received from the user of interest ($u = 1$) to estimate the transmitted bits. The performance of this signal is also compared to the same system in which the user of interest is allocated to use $1/4$ of the 1024 subcarriers but the other users are not present. Hence, from this study, we can discern the sole impact of simultaneously sending multiple PCM/FM-based CPM-OFDMA waveforms throught the AWGN channel. The results are shown in Fig. (4), where it is clear that the introduction of other users in this system does not impact the BER performance, as the orthogonality of the subcarriers allows the transmission of this PCM/FM-like signal by multiple users.

CONCLUSION

In this paper, we have first demonstrated that CPM-OFDMA schemes which are based on the PCM/FM, ARTM-CPM and SOQPSK-TG telemetry waveforms can provide similar performance over the AWGN channel when the sample rate $N \geq 2$. Interestingly, when $N = 1$, (which represents the most spectrally efficient scheme in terms of the number of required subcarriers per symbol interval) there can be a significant *improvement* in BER performance over conventional PCM/FM and ARTM-CPM. Secondly, a search for the best binary CPM-OFDMA schemes reveals that the lowest complexity schemes ($L = 2$, $N = 1$) offer better performance when compared to similarly defined CPM-OFDMA schemes ($L = 3$ and $L = 4$). Of all of the $L = 2$, $N = 1$ binary CPM-OFDMA schemes examined, the best performing achieves a BER of 10^{-6} at an E_b/N_0 of 7.8 dB. This can be compared with conventional PCM/FM (also binary, $L = 2$) which achieves a BER of 4×10^{-4} at the same E_b/N_0. In conclusion, CPM-OFDMA offers a robust, complementary modulation that can also be considered for use in aeronautical telemetry applications whenever frequency agility and spectral efficiency are compelling concerns.

REFERENCES

[1] C. Irving, "Range telemetry improvement and modernization," in *Proc. Int. Telemetering Conf.*, (Las Vega, NV), Oct. 1997.

[2] T. Hill, "An enhanced, constant envelope, interoperable shaped offset QPSK (SOQPSK) for improved spectral efficiency," in *Proc. Int. Telemetering Conf.*, (San Diego, CA), Oct. 2000.

[3] M. Goeghegan, "Description and performance results for the advanced range telemetry (artm) tier ii waveform," in *Proc. Int. Telemetering Conf.*, (San Diego, CA), pp. 90–96, Oct. 2000.

[4] T. Hill, "Performance of soqpsk and multi-h cpm in the presence of adjacent channel interference," in *Proc. Int. Telemetering Conf.*, (Las Vegas, NV), Oct. 2001.

[5] Range Commanders Council Telemetry Group, Range Commanders Council, White Sands Missile Range, New Mexico, *IRIG Standard 106-04: Telemetry Standards*, 2004. (Available on-line at http://www.ntia.doc.gov/osmhome/106.pdf).

[6] T. Frank, A. Klein, E. Costa, and E. Schulz, "Low complexity equalization with and without decision feedback and its application to IFDMA," in *Proc. IEEE International Symposium on Personal, Indoor and Mobile Radio Communications (PIMRC)*, vol. 2, pp. 1219–1223, Sep. 2005.

[7] J. B. Anderson, T. Aulin, and C.-E. Sundberg, *Digital Phase Modulation*. New York: Plenum Press, 1986.

[8] E. Perrins and M. Rice, "Reduced complexity approach to iterative detection of coded soqpsk," *IEEE Trans. Commun.*, vol. 55, 2007.

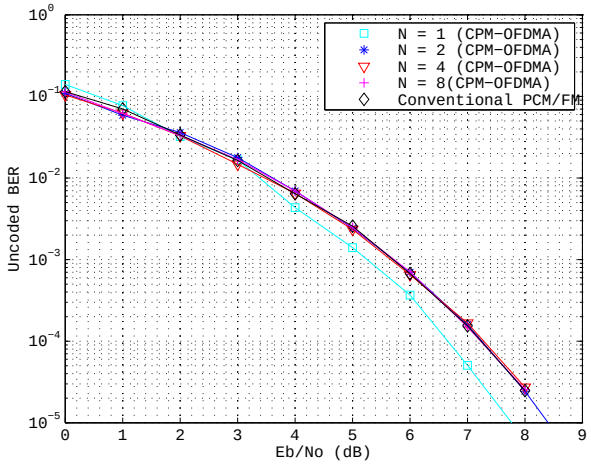

Figure 1: Performance of PCM/FM based schemes.

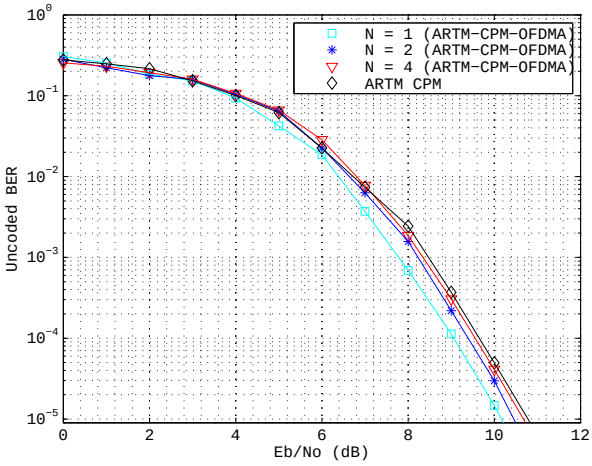

Figure 2: Performance of ARTM-CPM based schemes.

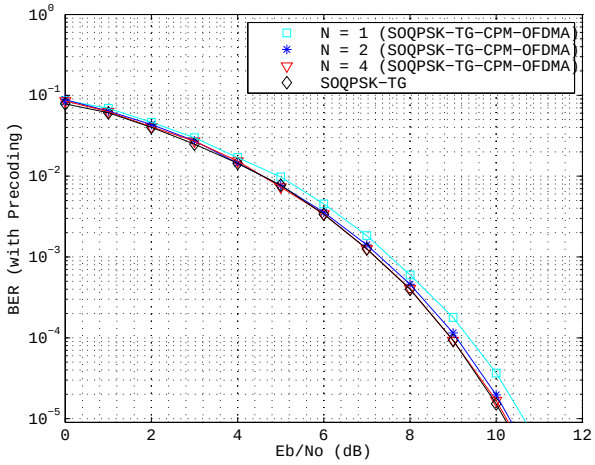

Figure 3: Performance of SQOPSK-TG-based schemes.

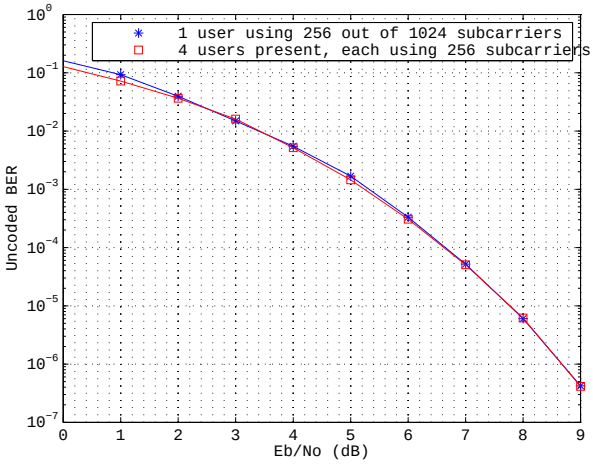

Figure 4: Multiuser PCM/FM based CPM-OFDMA.